JOURNAL OF GEOPHYSICAL RESEARCH, VOL. 92, NO. A1, PAGES 187–194, JANUARY 1, 1987

The Current-Voltage Relationship in Auroral Current Sheets

D. R. WEIMER,[1] D. A. GURNETT,[2] C. K. GOERTZ,[2] J. D. MENIETTI,[3]
J. L. BURCH,[3] AND M. SUGIURA[4]

The current-voltage relation within narrow auroral current sheets is examined through the use of high-resolution data from the high-altitude Dynamics Explorer 1 satellite. The north-south perpendicular electric field and the east-west magnetic field are shown for three cases in which there are large amplitude, oppositely directed paired electric fields which are confined to a region less than 20 km wide. The magnetic field variations are found to be proportional to the second integral of the high-altitude perpendicular electric field. It is shown that at the small-scale limit, this relationship between ΔB and E is consistent with a linear "Ohm's law" relationship between the current density and the parallel potential drop along the magnetic field line. This linear relationship had previously been verified for large-scale auroral formations greater than 20 km wide at the ionosphere. The evidence shown here extends our knowledge down to the scale size of discrete auroral arcs.

INTRODUCTION

In this paper we present high-resolution measurements obtained with the Dynamics Explorer 1 spacecraft within very narrow current sheets. The data suggest that a linear "Ohm's law" is valid for the current-voltage relation within current sheets which are just a few kilometers in thickness. In each case presented here the perpendicular electric fields have the structure of "electrostatic shocks," i.e., oppositely directed pairs with magnitudes over 100 mV/m. The structure of these "shocks" is seen to be a consequence of the auroral current-voltage relation.

Evidence for a linear Ohm's law relationship between field-aligned current and parallel potential drop had previously been found by *Lyons et al.* [1979] and *Menietti and Burch* [1981] on the basis of measurements of precipitating electron fluxes at the ionosphere. In these experiments the potential drops above the satellites were inferred from spectral plots of electron flux versus energy. The total energy fluxes were found to be proportional to the square of the potential drops. This implied that the current density is linearly proportional to the voltage. Lyons et al. had measured parallel field line conductances in the range of 1×10^{-10} to 9.6×10^{-10} mho/m^2. The linear Ohm's law relationship was also verified in a recent study by *Weimer et al.* [1985]. Rather than measure electron fluxes, the 1985 paper employed a different technique based on the spectral analysis of perpendicular electric fields which were measured nearly simultaneously by the two Dynamics Explorer satellites at different altitudes on auroral field lines. The currents were inferred from magnetic field measurements. Parallel field line conductances of the order of 10^{-8} mho/m^2 were measured.

Discussions on the theory of the auroral current-voltage relationship can be found in papers by *Knight* [1973], *Fridman and Lemaire* [1980], *Lyons* [1980, 1981], *Chiu and Cornwall* [1980], *Chiu et al.* [1981], and *Stern* [1981]. In general, expressions for the upward field-aligned current density due to electrons precipitating into the ionosphere are derived from calculations of free particle motion in a dipole magnetic field. The presence of a parallel electric field above the point where the magnetospheric electrons would normally be reflected by the magnetic mirror force causes a fraction of the electrons to be precipitated. While the exact expression relating current to potential drop is fairly complex, with some assumptions the relationship can be simplified to one showing that the current density is linearly proportional to the field-aligned potential drop. The "conductance" value depends on the density and thermal energy of the magnetospheric electrons and can be expressed as [*Lyons*, 1981]

$$G = \frac{e^2 n}{(2 m_e K_{th})^{1/2}} = 1.07 \times 10^{-23} \frac{n}{K_{th}^{1/2}} \frac{\text{mho}}{\text{m}^2} \qquad (1a)$$

given density and energy in MKS units. With density given in units of cm^{-3} and energy in eV the equivalent expression is

$$G = 2.7 \times 10^{-8} \frac{n}{K_{th}^{1/2}} \frac{\text{mho}}{\text{m}^2} \qquad (1b)$$

(In many papers the conductivity is referred to as K or the Lyons-Evans-Lundin constant.) With $n = 1$ cm^{-3} and $K_{th} = 250$ eV the conductance is 1.7×10^{-9} mho/m^2. For $n = 5$ cm^{-3} and $K_{th} = 100$ eV the conductance is 1.4×10^{-8} mho/m^2, so there appears to be a good theoretical justification for the aforementioned observations. However, there has been very little work done in the area of downward current regions, although *Stern* [1981] does include some discussion on this subject.

The kinetic theory calculations assume that a parallel electric field exists, without regard for how it is produced. Several mechanisms have been suggested as being responsible for producing the parallel electric fields, such as anomalous resistivity [*Papadopoulos*, 1977; *Falthammar*, 1977; *Hudson et al.*, 1978; *Lysak and Hudson*, 1979; *Lysak and Dum*, 1983], double layers [*Block*, 1978; *Goertz*, 1979], and the magnetic mirror effect [*Persson*, 1966; *Alfvén and Falthammar*, 1963; *Lemaire and Scherer*, 1974]. General discussions on the subject of parallel electric fields can be found in the reviews by *Shawhan et al.* [1978], *Mozer et al.* [1980], and *Stern* [1983].

There appears to be a link between parallel electric fields and the small-scale regions of very large perpendicular electric fields which were observed by *Mozer et al.* [1977]. There is evidence that these electrostatic shocks, which were measured

[1] Regis College Research Center, Weston, Massachusetts.
[2] Department of Physics and Astronomy, University of Iowa, Iowa City.
[3] Southwest Research Institute, San Antonio, Texas.
[4] Kyoto University, Kyoto, Japan.

Paper number 6A8528.
0148-0227/87/006A-8528$05.00

with the S3-3 satellite, are associated with discrete auroral arcs [*Torbert and Mozer*, 1978] and regions of upward–downward ion–electron acceleration [*Mozer et al.*, 1980; *Temerin et al.*, 1981].

The question has remained, What kind of current-voltage relation is there in these narrow regions (under 20 km wide at the ionosphere) where large-magnitude electric fields are found? The S3-3 satellite lacked a magnetic field measurement with sufficient spatial resolution to determine the current structure on the same size scale as the electric field [*Mozer et al.*, 1980]. The study by *Weimer et al.* [1985] had been limited to structures with spatial widths greater than 20 km at the base of the field lines. This 20-km limit had been imposed by the measurement of the electric field on the high-altitude DE 1 satellite, as the electric field in the spacecraft's orbit plane is measured with just one rotating double probe. A static electric field appears in the "raw" data as a sine wave with a 6-s period. The electric fields which had been used in the 1985 paper had been derived from a least square error fit of the signal to a sine wave. This fitting process works extremely well for measuring the large-scale electric fields which change on a time scale greater than the satellite spin period. But the rapid, small-scale variations, which usually have the largest magnitudes, are filtered out by this process. In order to obtain the electric field with a better spatial resolution, the sine wave modulation can be removed from the data in a more direct manner. In this paper we will show DE 1 electric field measurements with the highest possible resolution, and we will compare these electric fields to magnetic field measurements with the same time (spatial) resolution. The data show that an Ohm's law appears to be valid for current structures just a few kilometers across.

THEORY

First we will discuss what sort of relationship is to be expected (assuming an Ohm's law) between the north-south, perpendicular electric field and the east-west magnetic field variations. It is well known that just above the ionosphere, below the altitude of field-aligned electric fields, the height-integrated ionospheric Pedersen conductivity (Σ_p) is an important factor in the relationship between the field-aligned currents and the perpendicular electric fields. *Smiddy et al.* [1980] have shown that at the top of the ionosphere

$$j_{\parallel} = -\partial(E_x\Sigma_p)/\partial x \tag{2}$$

Here we use a coordinate system in which the Z axis is upward along the magnetic field line, X is southward, and Y is eastward. This quantity $j_{\parallel}$ is the magnetic field-aligned current density, which can be inferred from the derivative of the east-west magnetic field component measured on a satellite which is moving in the north-south direction. The currents are assumed to be in the form of "infinite sheets," i.e., much larger in the east-west and up-down directions than their width in the north-south direction. With this assumption, the magnetic and electric fields are related to each other according to

$$\Delta B_y = -\mu_0\Sigma_p E_x \tag{3}$$

where ΔB_y is the difference between the measured magnetic field and the earth's dipole field. Equation (3) has been confirmed by a number of measurements of magnetic and electric fields just above the ionosphere [*Smiddy et al.*, 1980; *Sugiura*, 1984]. At higher altitudes, (3) may not be valid due to the possible existence of an electric potential drop parallel to the magnetic field ($V_{\parallel}$). The Ohm's law we are investigating assumes that the field-aligned current density at the ionosphere and the parallel potential drop are related by

$$j_{\parallel} = -GV_{\parallel} \tag{4}$$

where G is the field line conductance. The sign convention is such that the current is positive (upward) when the potential decreases in going from low to high altitude, so that the potential drop, $V_{\parallel} = V_{\text{high}} - V_{\text{low}}$, is negative.

It is shown by *Weimer et al.* [1985] that with the definition of a constant inverse scale length or "critical wave number,"

$$G/\Sigma_p = k_0^2 \tag{5}$$

the Fourier transforms of the high-altitude quantities $j_{\parallel}$, B_y, and E_x have a relationship which depends on their spatial wave number k:

$$\tilde{j}_{\parallel} = \frac{-ik}{(k/k_0)^2 + 1}\Sigma_p\tilde{E}_x \tag{6}$$

$$\mu_0\tilde{j}_{\parallel} = ik\tilde{B}_y \tag{7}$$

The tildes indicate that the quantities are transformed from a spatial domain to a wave number domain. The spatial variations are presumed to be in the north-south (x) direction.

With a field line conductance of 10^{-8} mho/m^2 and a Pedersen conductance of 5 to 10 mho, the inverse of the critical wave number k_0^{-1} will be in the range of 22–32 km. The wavelength $\lambda_0 = 2\pi/k_0$ is 140–200 km. At the limit of a very small wavelength and large wave number, where $(k/k_0)^2 \gg 1$, (6) can be simplified to

$$\tilde{j}_{\parallel} = -(i/k)G\tilde{E}_x \tag{8}$$

From (4) we see that

$$-ik\tilde{V}_{\parallel} = \tilde{E}_x \tag{9a}$$

or in real space,

$$-\partial V_{\parallel}/\partial x = E_x \tag{9b}$$

where E_x is the measured electric field above the potential drop. Therefore at very small wavelengths the ionospheric conductivity does not influence the high-altitude electric field, and there is a very simple relationship between the north-

TABLE 1. DE 1 Position and Magnetic Field Line Mapping Factors (to 1 R_E) for Three Events

	Date, 1981		
	October 19 (day 292)	October 23 (day 296)	October 30 (day 303)
UT	0345:15	0345:04	1327:55
MLT	2031	2020	2039
Altitude, km	10,520	9,015	12,754
Radial distance, R_E	2.65	2.42	2.97
Perpendicular spacecraft velocity, km/s	4.77	5.31	4.34
Invariant latitude	69.39°	65.1°	67.27°
L Shell	8.07	5.64	6.70
North-south mapping factor	4.73	4.24	5.90
Area mapping factor	20.42	15.92	30.22

south electric field and the parallel potential drop. By integrating E_x one can obtain a "potential profile" ($V_{\parallel}$ as a function of x), which should be proportional to the current density if the Ohm's law of (4) is correct. Integration of E_x a second time (with multiplication by G and μ_0) should result in ΔB_y. This prediction can be tested by comparing E_x and ΔB_y in cases where the short wavelength variations are of large magnitude in comparison to the long wavelength variations.

While the analysis leading up to this conclusion is based on the assumption of uniform ionospheric conductivity, the same relationship between E_x and ΔB_y holds (at the small wavelength limit) if the conductivity is modified by precipitating electrons. One way to verify this is with a numerical calculation of ionospheric and high-altitude electric fields, given the field-aligned current as the input. With a constant conductivity and a sine wave current structure it is very easy to verify the analytical solution for the electric field ratios given in the paper by *Weimer et al.* [1985]. If the conductivity is then modified where the current is upward, by some function related to the current density, then the high-altitude electric field is changed at large wavelengths but is nearly identical to the constant conductivity case at small wavelengths.

OBSERVATIONS

Three examples of electric and magnetic fields from the high-altitude Dynamics Explorer 1 satellite are presented here. Table 1 contains a summary of the three event locations and field line mapping factors. The common feature of the three events is the presence of large-magnitude, oppositely directed electric fields confined to a narrow region of space. The cases for study were selected from a very limited set of data from early in the DE mission. High-resolution magnetometer data were compared to the electric field for only seven cases where large electric fields were found. Shown here are the cases where there is a good correlation between ΔB and E. In three cases where there was no apparent relationship the electric field structures were about three times wider; the requirement that $(k/k_0)^2 \gg 1$ does appear to be important. In another case large variations in all three magnetic field components indicated that the current was not in the form of a thin stationary sheet.

The electric field in the orbit plane of the DE 1 satellite is measured with a double-probe antenna measuring 200 m tip to tip. The electric field is sampled at a rate of 16 samples/s by the plasma wave instrument. The complete instrument description is given by *Shawhan et al.* [1981]. The "raw" electric field is modulated by the satellite's rotation, which has a 6-s period. With the assumption that the electric field is perpendicular to the magnetic field, the spin modulation can be removed by dividing each measurement by the sine of the angle between the double-probe antenna and the magnetic field in the spin plane. This demodulation procedure works well when the "spin phase angle" is large, but when the antenna is nearly parallel to the magnetic field there can be problems: a small error in the phase angle results in a distorted electric field, which goes to infinity when the angle is zero. To eliminate this effect gaps are introduced in the despun data whenever the magnitude of the phase angle is less than 30°.

The top panel in Figure 1 shows 30 s of high-resolution electric field data which has had the spin modulation removed by this technique. As subsequent steps in the data analysis require a continuous electric field, the gaps have been filled in

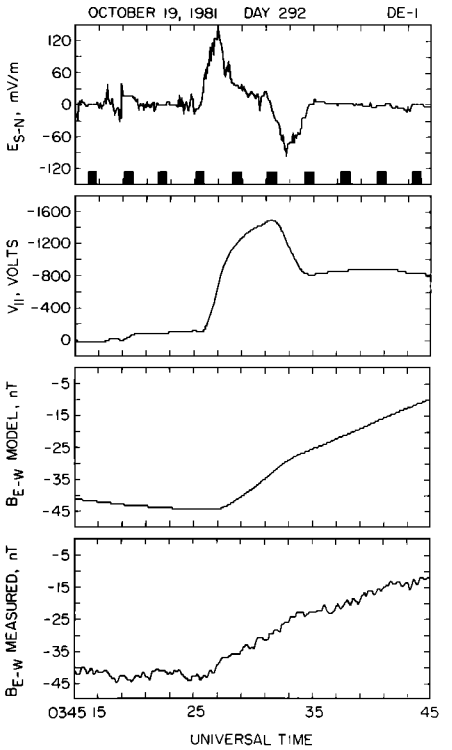

Fig. 1. Electric and magnetic fields measured with DE 1 in the 30-s interval from 0345:15 to 0345:45 UT on October 19 (day 292), 1981. Top graph is the north-south electric field measured in the orbit plane. Data has had the spin modulation removed; the blocks above the time axis indicate where "gaps" have been filled in. Second graph shows the potential obtained by integrating this electric field, and the third graph shows a model of the east-west magnetic field obtained by a second integration. At the bottom is shown the measured magnetic field. A positive slope is indicative of passage through an upward current. DE 1 spacecraft was moving north to south in the northern hemisphere at this time.

with values which smoothly connect the data on both sides of the gaps. The time axis on the plot has been marked with shaded blocks to indicate where these gaps occur. The resulting graph shows a large-amplitude electric field which points southward for 6.0 s then reverses to a northward direction for 3.5 s. At the time of this measurement the velocity component of DE 1 perpendicular to the magnetic field was 4.77 km/s in a southward direction; therefore the total width of this structure is 45 km. The satellite was located at a radial distance of 2.65 R_E on a magnetic field line with a McIlwain parameter (L) equal to 8.07. Since the north-south separation of field lines maps according to

$$\frac{\Delta x(r, L)}{\Delta x(1, L)} = \left(\frac{4L - 3}{4L - 3r}\right)^{1/2} r^{3/2} \tag{10}$$

then 45 km maps to a width of 9.5 km at the base of the magnetic field line.

Integration of the electric field in Figure 1 results in the electric potential function which is shown in the second plot from the top in the same figure. The integration is done by adding each data point to a sum, after multiplication by the appropriate time and velocity constants. Multiplication of the potential by a conductance results in a value for the local current density; the integration of this current density, equivalent to the second integral of the electric field, results in the east-west deviation of the magnetic field shown in the third

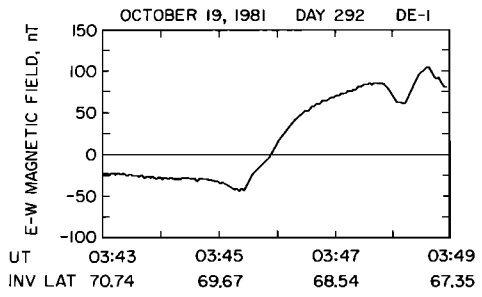

Fig. 2. East-west magnetic field component from the magnetometer on DE 1 for the time period from 0343 to 0349 UT on October 19 (day 292), 1981. Earth's dipole field has been subtracted from the measured values.

plot. The bottom plot in Figure 1 shows the actual value of the east-west magnetic field measured with the magnetometer on DE 1 [*Farthing et al.*, 1981]. This magnetic field, which is also sampled at 16 data points/s, has had the background field due to the earth's dipole subtracted, leaving only perturbations due to the satellite's motion through currents. High-frequency noise has been removed with a five-point moving average filter.

Figure 1 shows a very good match between the second integral of the electric field and the measured magnetic field. To obtain such a good agreement a trial-and-error adjustment of two parameters was necessary. These parameters are an offset potential and the field-line conductance. The potential in Figure 1 is shown to start at zero; a constant voltage may be added to compensate for the actual initial value. An offset of +200 V, added before the second integration, yielded the best match with the magnetic field. This positive potential at the high-altitude location should correspond to a downward current. Figure 2, which shows the measured east-west magnetic field for a longer time interval, indicates that the addition of a positive potential is justified. Prior to the electric field spike at 0345:25 UT there was a gradual negative (westward) slope in the magnetic field, which corresponds to a downward current. The large electric fields are located on the boundary between this downward current and a broad upward current region. A narrow but large magnitude upward current sheet is located right on the boundary. This peak in the upward current occurs precisely at the point where the high-altitude potential is most negative.

The addition of a constant to the potential is equivalent to adding a constant slope to the second integral (model magnetic field). The magnitudes of the relative changes in the magnetic field are determined by the value chosen for the field line conductance. In this case a conductance of 4×10^{-10} mho/m^2 yielded the best match between the model and measured magnetic field. With this value of the conductance the local current density is figured to be 5.2×10^{-7} A/m^2 at the point where the potential drop is -1300 V. Due to the convergence of the magnetic flux tubes, the current density increases toward lower altitudes. The flux tube area mapping factor to 1 R_E is

$$\frac{\Delta A(r, L)}{\Delta A(1, L)} = \left(\frac{4L - 3}{4L - 3r}\right)^{1/2} r^3 \qquad (11)$$

For this case the mapping factor is 20.42, so the "normalized" field line conductance is 8.2×10^{-9} mho/m^2. This is the ratio between the current density at the base of the field line (1.1×10^{-5} A/m^2) and the total potential drop along the field line (1.3 kV). However, if there is an additional potential drop above the satellite then this measurement of the total potential is too low and the estimate for the conductivity is too high.

For this case from October 19 (day 292), 1981, it is instructive to examine the data from the high altitude plasma instrument (HAPI) on DE 1. The instrument description is in the paper by *Burch et al.* [1981]. In Figure 3 are shown a sequence of electron and ion distribution functions measured with the HAPI from 0345:12 to 0345:48 UT. Each distribution function is derived from data collected by the instrument during two complete rotations of the spacecraft. There are very distinct changes in the distribution functions as the spacecraft moves across the region with the large electric fields. Initially, the distribution functions are rather symmetrical; after crossing the region where the high-altitude potential goes from positive to negative, there is evidence of ions which have been accelerated up the field lines and a wide electron loss cone, indicative of a parallel electric field below the spacecraft. These changes in the distribution functions were coincident with the entry of DE 1 into the boundary plasma sheet (the sudden increase in electron temperature is more obvious in a color energy-time spectrogram of the electron distribution function, not shown here).

There are indications of ions moving upward with the energies predicted by the electric potential, such as the contour "island" at $v_{\parallel} = -470$ km/s (1200 eV) from 0345:24.6 to 0345:36.6 UT. However, a greater number of ions appear to have been accelerated to higher energies (up to 3 keV). This puzzle is perhaps related to the observations by *Mizera et al.* [1981] and *Collin et al.* [1981] of O^+ ions being more energetic than the H^+ ions. The distribution functions shown in Figure 3 are for all ions, as the energies are measured without a distinction between species. On the other hand, the electron loss cones appear to be in better agreement with the potential drop obtained from the electric field. The very wide loss cone from 0345:24.6 to 0345:36.6 UT corresponds to a potential drop of about 1400 V; in the distribution function for the next time interval the loss cone is more narrow, corresponding to about 600 V. These are only ball park figures, as the loss cone calculation depends on the altitude at which the parallel electric field is assumed to be located.

After 0345:36.7 UT there does not appear to be a significant potential drop above the satellite, as indicated by the absence of accelerated electrons moving down the field line. However, within the short-duration "shock," where the current is most intense, there may be downward moving electrons which could not be resolved by the plasma instrument. Since the instrument must step through the various energy channels while the spacecraft is rotating, short-duration changes in the distribution function will produce unreal artifacts in the contour plots, such as the clam shell edge in the middle plot. There may well have been an additional potential drop above the satellite at this point, resulting in an overestimate of the conductance.

Another case for study is shown in Figure 4. The data is from October 23 (day 296), 1981. The format is the same as in Figure 1. This event has some similarities to the previous case, yet there are important differences. Figure 5 shows that like before, the electric field "spike" occurred on the southward edge of a region of downward current. But this time the downward current is much larger in magnitude and confined to a

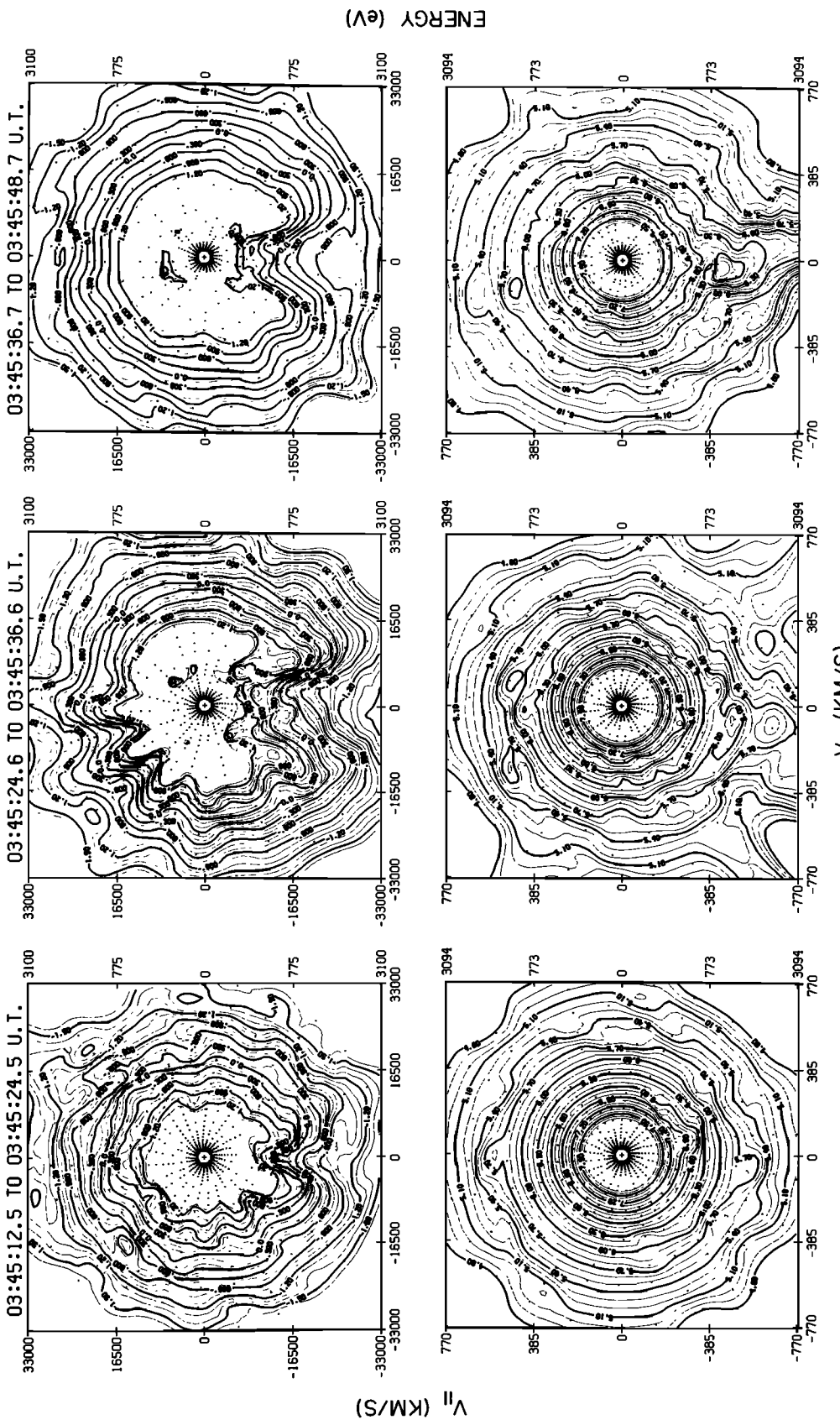

Fig. 3. Phase-space contours of the logarithm of the electron (top row) and ion (bottom row) distribution functions measured by DE 1 from 0345:12.5 to 0345:36.7 UT on October 19 (day 292), 1981. Each 12-s segment spans two spacecraft spin periods. Ion energies were measured with no distinction between species. Ion velocity scale is indicated for H^+ ions.

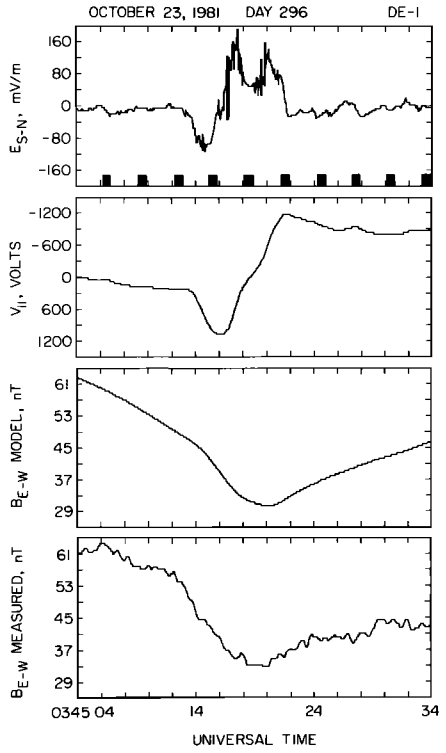

Fig. 4. Electric and magnetic fields measured with DE 1 in the time period from 0345:04 to 0345:34 UT on October 23 (day 296), 1981. Format is the same as in Figure 1.

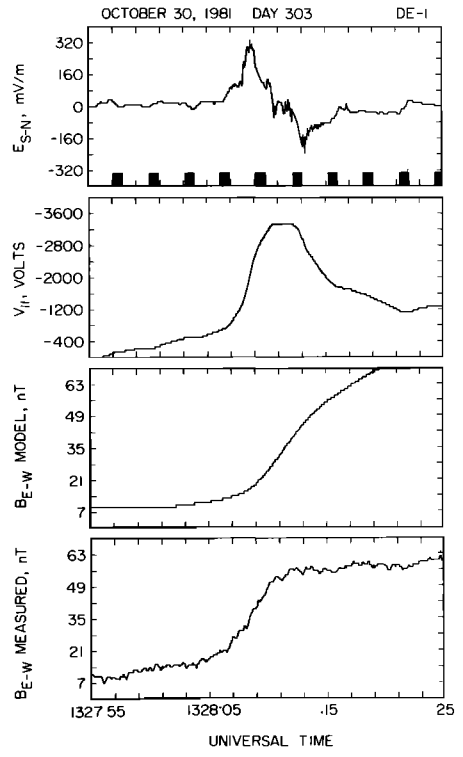

Fig. 6. Electric and magnetic fields measured with DE 1 in the time period from 1327:55 to 1328:25 UT on October 30 (day 303), 1981. Format is the same as in Figure 1.

relatively narrow region, embedded within a larger region of upward current (*Lin et al.* [1985] show large-scale "inverted-V" regions on both sides of this same event in their plate 1). Whereas in the previous case most of the magnetic field variations were due to upward currents, in this second example the downward currents are equally important.

As before, different parameters were tested in order to find a model magnetic field which best matched the measured field. In this case the most reasonable results were obtained with the addition of a +3 mV/m offset to the electric field before doing the first integration. This compensated for a negative (northward), large-scale convection electric field which would be linearly proportional to ΔB according to (3). A +500-V offset was added to the potential before doing the second integration. This is justifiable on the basis that the region of downward current had been penetrated a few seconds before the starting time of Figure 4. A conductance of 4×10^{-10} mho/m^2 was used to generate the model magnetic field. The DE 1 satellite was at a distance of 2.415 R_E and at an invariant latitude of 65.1°, so the current projection factor to the field line base is 15.92. This results in a normalized field line conductance of 6.4×10^{-9} mho/m^2.

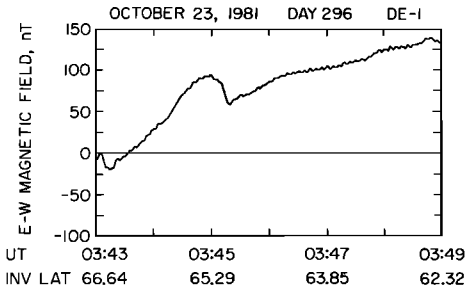

Fig. 5. East-west magnetic field component from the magnetometer on DE 1 for the time period from 0343 to 0349 UT on October 23 (day 296), 1981.

The final example is shown in Figure 6, from October 30 (day 303), 1981. In this case the match between the second integral of the electric field and the measured magnetic field is not as good as in the previous examples. A potential offset of +200 V and a conductance of 4×10^{-10} mho/m^2 were used to generate the second integral shown in Figure 6. Figure 7 shows that just like the previous cases, the large perpendicular electric fields are located in the edges of a narrow but very intense current sheet which is located on a boundary between large-scale downward and upward currents. The main difference between this and the previous cases is that the magnitudes are greater: the electric field reaches 320 mV/m, the potential exceeds 3 kV, and the current density is greater than 1.2×10^{-6} A/m^2 (the ionospheric current density is 30.22 times higher). The "model" magnetic field is very much similar to the measured field up to 1311 UT, after which the measured field levels off and the integrated value continues to increase. A higher conductance of 7×10^{-10} mho/m^2 (with a normalized value of 2.1×10^{-8} mho/m^2) makes a better match for the period up to 1311 UT, but after that point a higher conductance makes the disagreement worse. The problem may be due to inaccurate electric fields in the data gaps. Alternatively, the field line conductance might not have been constant throughout this region.

Discussion and Summary

The evidence which has been shown here provides a convincing case for the validity of (4) within current sheets with small spatial widths. The linear relationship between current density and potential is the simplest explanation for the mag-

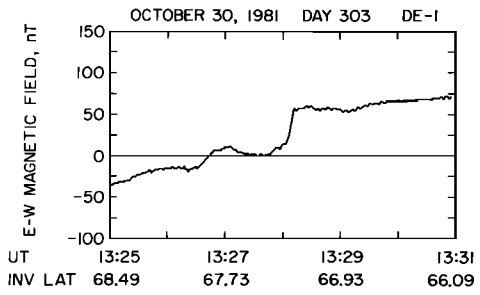

Fig. 7. East-west magnetic field component from the magnetometer on DE 1 for the time period from 1325 to 1331 UT on October 30 (day 303), 1981.

netic field signatures which are observed concurrent with the large-amplitude electric fields. In general, the large-amplitude perpendicular electric fields occur on the edge of large-magnitude current sheets or on the boundary between upward and downward currents, where the high-altitude potential must make a large jump within a short distance. The potential difference between the magnetosphere and ionosphere needs to adjust itself in order that the currents flow in proportion to the difference, in the direction from high to low potential.

The changes in the ionospheric potential due to the convection electric field are a very important factor in the large-scale pattern of field-aligned currents. In general, it would not be valid to make a determination of the field-aligned potential drop based on just a measurement of the high altitude electric field. However, we have shown here that within current sheets with very small "wavelengths" the ionospheric potential may be treated as a constant.

A theory based on a linear Ohm's law shows that for the small-scale features the second integral of the north-south electric field should be proportional to the east-west magnetic field variations. The data which have been shown here support this theory. In order to show the good agreements between the second integral of the measured electric field and the measured magnetic field it was necessary to adjust two unknown quantities: the potential offset and the field-aligned conductance. These adjustments were within reason and relatively minor. The second integral would not have given the observed agreement if the Ohm's law was not a good approximation. Indeed, given the gaps in the electric field data it is amazing that the integrated values come as close as they do to matching the measured magnetic fields, since the integrations cause errors to accumulate forward in time.

The normalized field line conductances determined with this technique generally are in the range of 10^{-8} to 10^{-9} mho/m^2. This conductance is within the limits of the kinetic theory (equation (1)), although *Fridman and Lemaire* [1980] predict typical values which are smaller by a factor of 10. Perhaps more critical is the fact that the functional form of the current-voltage relation depends upon the ratio of B_i/B_v, the magnetic field strength at the ionosphere divided by the magnetic field strength at the top of the voltage drop. Fridman and Lemaire show that the linear approximation holds only for a limited range of $V_{\|}$. They require that $1 \ll eV_{\|}/K_{th} \ll B_i/B_v$. For the three cases shown here the magnetic field ratio at the point of observation is only in the range of 16–30. If K_{th} is in the range of 100–250 eV then the limits on $V_{\|}$ are satisfied only for potentials greater than 100–250 V and less than 1600 to 4000 V. Our comparisons between ΔB and the second integral of E may work so well only because the potentials jump rather quickly past the lower limit and do not exceed the upper limit, with the exception of the third case where the match to the model was the poorest. It is also possible that in all three cases the parallel electric field extends to altitudes above the satellite, where B_i/B_v is much higher. In that case the potential measured at the satellite altitude is a fraction of the total potential difference.

There is still the question of which of the proposed mechanisms is responsible for creating the field-aligned electric fields. Evidence in favor of the magnetic mirror effect (hot electrons and ions mirror at different points on field lines, causing charge separation) as the source of a parallel potential drop is found in the first case shown here, as the potential jumped suddenly when DE 1 entered the plasma boundary sheet. However, the kinetic theory works in one direction only, for upward currents due to downward precipitating electrons. In the second example we have shown (Figure 4) the conductance appears to be the same for both upward and downward currents. This is a very puzzling result. In every case short wavelength "turbulence" in the electric field is present where the currents are most intense, suggesting that large-amplitude plasma waves may be associated with the currents. Anomalous resistivity may be important. Wave particle interactions might also explain how some ions get accelerated to energies higher than the measured potential drop.

From these data it is not possible to tell how the potential drop is distributed along the field lines. Abrupt jumps in the form of double layers may well be present. Our results do not contradict the stationary V-shaped and S-shaped electric equipotential models which are shown in the papers by *Hudson and Mozer* [1978] and *Mozer et al.* [1980]. The three events shown here are good examples of cases where S-shaped contours could be present; i.e., the shocks are associated with a boundary between upward and downward currents. This type appears to be the most common, although a "pure" S shock has an electric field in one direction only and the events shown here have reversing fields. In the second case (Figure 4) the large electric fields are found on one edge of a downward current region which is nested between a larger region of upward current; the overall structure is like a V-shaped contour.

Finally, we address the "chicken and egg" problem of the origin of the field-aligned currents and potential drops. This is equivalent to asking if the source is a current or voltage generator. *Lysak* [1985] has shown that small-scale structures are more consistent with current generators. The data shown here suggest that this is the case; the large-magnitude electric fields which are found at high altitudes do not form by themselves and subsequently drive the current. Instead, wherever current sheets are formed nature finds a way to make self-consistent adjustments so that the current flow is in proportion to a potential difference between the magnetosphere and ionosphere. Small-scale features require that the divergence of the high-altitude potential be large, resulting in the large-magnitude electric fields with a shocklike structure.

Acknowledgments. The research at the University of Iowa was supported by NASA through grants NAG5-310, NGL-16-001-002, and NGL-16-001-043, and by the Office of Naval Research through contract N00014-85-K-0183. The research at Southwest Research Institute was supported by NASA through contract NAS5-28711. The research at Regis College was supported by U.S. Air Force contract F19628-84-C-0126.

The Editor thanks D. Evans and M. Temerin for their assistance in evaluating this paper.

REFERENCES

Alfvén, H., and C.-G. Falthammar, *Cosmical Electrodynamics*, 2nd ed., Oxford University Press, New York, 1963.

Block, L. P., A double layer review, *Astrophys. Space Sci., 55*, 59, 1978.

Burch, J. L., J. D. Winningham, V. A. Blevins, N. Eaker, W. C. Gibson, and R. A. Hoffman, High-altitude plasma instrument for Dynamics Explorer-A, *Space Sci. Instrum., 5*, 455, 1981.

Chiu, Y. T., and J. M. Cornwall, Electrostatic model of a quiet auroral arc, *J. Geophys. Res., 85*, 543, 1980.

Chiu, Y. T., A. L. Newman, and J. M. Cornwall, On the structure and mapping of auroral electrostatic potentials, *J. Geophys. Res., 86*, 10029, 1981.

Collin, H. L., R. D. Sharp, E. G. Shelley, and R. G. Johnson, Some general characteristics of upflowing ion beams over the auroral zone and their relationship to auroral electrons, *J. Geophys. Res., 86*, 6820, 1981.

Falthammar, C.-G., Problems related to macroscopic electric fields in the magnetosphere, *Rev. Geophys. Space Phys., 15*, 457, 1977.

Farthing, W. H., M. Sugiura, B. G. Ledley, and L. J. Cahill, Magnetic field observations on DE A and B, *Space Sci. Instrum., 5*, 551, 1981.

Fridman, M., and J. Lemaire, Relationship between auroral electron fluxes and field aligned electric potential differences, *J. Geophys. Res., 85*, 664, 1980.

Goertz, C. K., Double layers and electrostatic shocks in space, *Rev. Geophys. Space Phys., 17*, 418, 1979.

Hudson, M. K., and F. S. Mozer, Electrostatic shocks, double layers, and anomalous resistivity in the magnetosphere, *Geophys. Res. Lett., 5*, 131, 1978.

Hudson, M. K., R. L. Lysak, and F. S. Mozer, Magnetic field-aligned potential drops due to electrostatic ion cyclotron turbulence, *Geophys. Res. Lett., 5*, 143, 1978.

Knight, S., Parallel electric fields, *Planet. Space Sci., 21*, 741, 1973.

Lemaire, J., and M. Scherer, Ionosphere-plasmasheet field-aligned currents and parallel electric fields, *Planet Space Sci., 22*, 1485, 1974.

Lin, C. S., J. N. Barfield, J. L. Burch, and J. D. Winningham, Near-conjugate observations of inverted-V electron precipitation using DE 1 and DE 2, *J. Geophys. Res., 90*, 1669, 1985.

Lyons, L. R., Generation of large-scale regions of auroral currents, electric potentials, and precipitation by divergence of the convection electric fields, *J. Geophys. Res., 85*, 17, 1980.

Lyons, L. R., Discrete aurora as the direct result of an inferred high-altitude generating potential distribution, *J. Geophys. Res., 86*, 1, 1981.

Lyons, L. R., D. S. Evans, and R. Lundin, An observed relation between magnetic field-aligned electric fields and downward electron energy fluxes in the vicinity of auroral forms, *J. Geophys. Res., 84*, 457, 1979.

Lysak, R. L., Auroral electrodynamics with current and voltage generators, *J. Geophys. Res., 90*, 4178, 1985.

Lysak, R. L., and C. T. Dum, Dynamics of magnetosphere-ionosphere coupling including turbulent transport, *J. Geophys. Res., 88*, 365, 1983.

Lysak, R. L., and M. K. Hudson, Coherent Anomalous Resistivity in the region of electrostatic shocks, *Geophys. Res. Lett., 6*, 661, 1979.

Menietti, J. D., and J. L. Burch, A satellite investigation of energy flux and inferred potential drop in auroral electron energy spectra, *Geophys. Res. Lett., 8*, 1095, 1981.

Mizera, P. F., et al., The aurora inferred from S3 3 particles and fields, *J. Geophys. Res., 86*, 2329, 1981.

Mozer, F. S., C. W. Carlson, M. K. Hudson, R. B. Torbert, B. Parady, and J. Yatteau, Observations of paired electrostatic shocks in the polar magnetosphere, *Phys. Rev. Lett., 38*, 292, 1977.

Mozer, F. S., C. A. Cattell, M. K. Hudson, R. L. Lysak, M. Temerin, and R. B. Torbert, Satellite measurements and theories of low altitude auroral particle acceleration, *Space Sci. Rev., 27*, 155, 1980.

Papadopoulos, K., A review of anomalous resistivity of the ionosphere, *Rev. Geophys. Space Phys., 15*, 113, 1977.

Persson, H., Electric fields parallel to the magnetic field in a low-density plasma, *Phys. Fluids, 9*, 1090, 1966.

Shawhan, S. D., C.-G. Falthammar, and L. P. Block, On the nature of large auroral zone electric fields at 1 R_E altitude, *J. Geophys. Res., 83*, 1049, 1978.

Shawhan, S. D., D. A. Gurnett, D. A. Odem, R. A. Helliwell, and C. G. Park, The plasma wave instrument and quasi-static electric field instrument (PWI) for Dynamics Explorer-A, *Space Sci. Instrum., 5*, 535, 1981.

Smiddy, M., W. J. Burke, M. C. Kelley, N. A. Saflekos, M. S. Gussenhoven, D. A. Hardy, and F. J. Rich, Effects of high-latitude conductivity on observed convection electric fields and Birkeland currents, *J. Geophys. Res., 85*, 6811, 1980.

Stern, D. P., One-dimensional models of quasi-neutral parallel electric fields, *J. Geophys. Res., 81*, 5839, 1981.

Stern, D. P., Electric currents and voltage drops along auroral field lines, *Space Sci. Rev., 34*, 317, 1983.

Sugiura, M., A fundamental magnetosphere-ionosphere coupling mode involving field-aligned currents as deduced from DE 2 observations, *Geophys. Res. Lett., 11*, 9, 877, 1984.

Temerin, M., C. Cattell, R. Lysak, M. Hudson, R. B. Torbert, F. S. Mozer, R. D. Sharp, and P. M. Kintner, The small-scale structure of electrostatic shocks, *J. Geophys. Res., 86*, 11278, 1981.

Torbert, R. B., and F. S. Mozer, Electrostatic shocks as the source of discrete auroral arcs, *Geophys. Res. Lett., 5*, 135, 1978.

Weimer, D. R., C. K. Goertz, D. A. Gurnett, N. C. Maynard, and J. L. Burch, Auroral zone electric fields from DE 1 and 2 magnetic conjunctions, *J. Geophys. Res., 90*, 7479, 1985.

J. L. Burch, Southwest Research Institute, P.O. Drawer 28510, San Antonio, TX 78284.

C. K. Goertz and D. A. Gurnett, Department of Physics and Astronomy, University of Iowa, Iowa City, IA 52242.

J. D. Menietti, Southwest Research Institute, P.O. Drawer 28510, San Antonio, TX 78284.

M. Sugiura, Kyoto University, Kyoto, Japan.

D. R. Weimer, Regis College Research Center, 235 Wellesley Street, Weston, MA 02193.

(Received April 29, 1986;
revised August 15, 1986;
accepted August 26, 1986.)